



International Journal of Bifurcation and Chaos, Vol. 25, No. 5 (2015) 1530014 (16 pages)
 © World Scientific Publishing Company
 DOI: 10.1142/S0218127415300141

Spatiotemporal Dynamics of a Diffusive Leslie–Gower Predator–Prey Model with Ratio-Dependent Functional Response*

Hong-Bo Shi

*School of Mathematical Science, Huaiyin Normal University,
 Huaian, Jiangsu 223300, P. R. China*

Shigui Ruan[†]

*Department of Mathematics, University of Miami,
 Coral Gables, FL 33124-4250, USA
 ruan@math.miami.edu*

Ying Su

*Department of Mathematics, Harbin Institute of Technology,
 Harbin, Heilongjiang 150001, P. R. China*

Jia-Fang Zhang

*School of Mathematics and Information Science,
 Henan University, Kaifeng, Henan 475001, P. R. China*

Received April 21, 2014; Revised January 4, 2015

This paper is devoted to the study of spatiotemporal dynamics of a diffusive Leslie–Gower predator–prey system with ratio-dependent Holling type III functional response under homogeneous Neumann boundary conditions. It is shown that the model exhibits spatial patterns via Turing (diffusion-driven) instability and temporal patterns via Hopf bifurcation. Moreover, the existence of spatiotemporal patterns is established via Turing–Hopf bifurcation at the degenerate points where the Turing instability curve and the Hopf bifurcation curve intersect. Various numerical simulations are also presented to illustrate the theoretical results.

Keywords: Diffusive predator–prey model; functional response; stability; Turing instability; Hopf bifurcation; Turing–Hopf bifurcation.

1. Introduction

Understanding the nonlinear dynamics of predator–prey systems and determining how the dynamical behaviors change along model parameters is an important subject in theoretical ecology. Because

of the differences in capturing food and consuming energy, a major trend in theoretical work on predator–prey dynamics has been launched so as to derive more realistic models and functional responses. Consider the following Leslie–Gower

*Research was partially supported by National Natural Science Foundation of China (Nos. 11461040, 11401245, 11301147 and 11201096), Universities Natural Science Foundation of Jiangsu Province (11KJB110003), and National Science Foundation (DMS-1412454).

[†]Author for correspondence

type predator–prey model [Hsu & Huang, 1995]:

$$\begin{cases} \frac{du}{dt} = r_1 u \left(1 - \frac{u}{K}\right) - p(u)v, \\ \frac{dv}{dt} = r_2 \left(1 - \frac{v}{hu}\right), \end{cases} \quad (1)$$

where u , v and r_1 , r_2 represent prey and predator densities and intrinsic growth rates, respectively. K is the carrying capacity of prey’s environment, while the carrying capacity of predator’s environment, hu , is a function on the population size of prey (h/r_2 is a measure of the food quality of the prey for conversion into predator growth). The form of the predator equation in system (1) was first introduced by Leslie [1948]. The function $\frac{v}{hu}$ is called the Leslie–Gower term [Leslie & Gower, 1960].

The functional response $p(u)$ can be classified into different types [Collings, 1997]. (i) Lotka–Volterra type: $p(u) = cu$, where $c > 0$ is the conversion rate of predators. System (1) with the Lotka–Volterra type functional response is the so-called Leslie–Gower model [Leslie & Gower, 1960]. (ii) Holling type II or Michaelis–Menten type [Holling, 1965]: $p(u) = \frac{cu}{m+u}$, where $m > 0$ is the half-saturation constant. The Leslie–Gower type predator–prey model (1) with Holling type II functional response is also called the Holling–Tanner model in the literature [May, 1973; Murray, 1989]. (iii) Holling type III [Bazykin, 1998; Smith, 1974]: $p(u) = \frac{cu^2}{m+u^2}$. Hsu and Huang [1995] obtained some criteria for the local asymptotic stability of the positive equilibrium of system (1) with Holling type III functional response and gave conditions under which local stability of the positive equilibrium implies global stability by applying Dulac criterion and constructing Lyapunov functions. (iv) Holling type IV: $p(u) = \frac{cu}{m+u^2}$, which is nonmonotonic. Li and Xiao [2007] studied system (1) with Holling type IV functional response and performed detailed qualitative and bifurcation analyses, such as the classification of equilibria, Hopf bifurcation, Bogdanov–Takens bifurcation, and stable/unstable limit cycles.

The functional responses mentioned above are only prey-dependent. Recent biological and physiological evidence [Arditi & Ginzburg, 1989; Arditi *et al.*, 1991; Arditi & Saiah, 1992] indicates that in many situations, especially when predators have to search for food (and therefore, have to share or compete for food), a more suitable general

predator–prey theory should be based on the fact that the per capita predator growth rate should be a function of the ratio of prey to predator abundance, the so-called ratio-dependent functional response. Xiao and Ruan [2001] considered a predator–prey model with ratio-dependent Holling type II functional response and provided global qualitative analysis of the model depending on all parameters and conditions of existence and nonexistence of limit cycles for the model. Ruan *et al.* [2010] further studied the same predator–prey model as in [Xiao & Ruan, 2001] and constructed the unfolding and proved its versatility and degeneracy of codimension-two. They discussed all its possible bifurcations, including transcritical bifurcation, Hopf bifurcation, and heteroclinic bifurcation, gave conditions of parameters for the appearance of closed orbits and heteroclinic loops, and described the bifurcation curves. For more studies on predator–prey systems with ratio-dependent Holling type-II functional response, we refer to [Freedman & Mathsen, 1993; Hsu *et al.*, 2001; Kuang, 1999; Kuang & Beretta, 1998; Li & Kuang, 2007; Liang & Pan, 2007; Ruan *et al.*, 2008, 2010; Xiao & Ruan, 2001].

On the other hand, in the evolutionary process of the species, the individuals do not remain fixed in space, and their spatial distribution changes continuously due to the impact of many reasons (environment factors, food supplies, etc.). Therefore, different spatial effects have been introduced into population models, such as diffusion and dispersal. For example, it has been known since Turing’s classical work [Turing, 1952] that the interplay of chemical reaction and diffusion can cause the stable equilibrium of the local system to become unstable for the diffusive system and lead to the spontaneous formulation of a spatially periodic stationary structure. In particular, this kind of instability is called Turing instability [Murray, 1989] or diffusion-driven instability [Okubo, 1980]. The space-dependent stationary solutions induced by diffusion are called Turing pattern. For reviews and related studies on Turing instability and Turing pattern formation of reaction–diffusion (R–D) systems from applied sciences such as chemistry, biology, ecology and epidemiology, we refer to [Du *et al.*, 2009; Gambino *et al.*, 2013; Golovin *et al.*, 2008; Levin & Segel, 1985; Li *et al.*, 2013; Malchow *et al.*, 2008; Peng, 2013; Peng & Wang, 2008; Ruan, 1998; Wang, 2008; Yi *et al.*, 2009; Zhang *et al.*, 2011], and references cited therein.

Recently, studies of dynamics resulting from the coupling between two different instabilities, Turing instability and Hopf instability (or bifurcation), have become available. Particularly, in some biological and chemical reaction–diffusion models, focus has been put on the coupling between instabilities breaking temporal and spatial symmetries, respectively. For example, Wang *et al.* [2007] investigated the emergence of a diffusive ratio-dependent predator–prey system with Holling type II functional response and obtained conditions of Hopf, Turing, and wave bifurcations in a spatial domain. Furthermore, they presented a theoretical analysis of evolutionary processes that involves organisms distribution and their interaction of spatially distributed population with local diffusion. For more related works, see [Baurmann *et al.*, 2007; Camara & Aziz-Alaoui, 2009; Meixner *et al.*, 1997; Wit *et al.*, 1996; Tzou *et al.*, 2011, 2013].

Motivated by the previous works, in this paper by incorporating the diffusion and ratio-dependent Holling type III functional response into system (1), we consider the following partial differential equation (PDE) model under homogeneous Neumann boundary conditions:

$$\begin{cases} \frac{\partial u}{\partial t} - d_1 \Delta u = r_1 u \left(1 - \frac{u}{K}\right) - \frac{cu^2v}{u^2 + mv^2}, & x \in \Omega, \quad t > 0, \\ \frac{\partial v}{\partial t} - d_2 \Delta v = r_2 v \left(-\frac{v}{hu}\right), & x \in \Omega, \quad t > 0, \\ \frac{\partial u}{\partial \nu} = \frac{\partial v}{\partial \nu} = 0, & x \in \partial\Omega, \quad t > 0, \\ u(x, 0) = u_0(x) \geq 0, & x \in \Omega, \\ v(x, 0) = v_0(x) \geq 0, & x \in \Omega. \end{cases} \quad (2)$$

Here, $u(x, t)$ and $v(x, t)$ stand for the densities of the prey and predators at location $x \in \Omega$ and time t , respectively; $\Omega \subset \mathbb{R}^N$ ($N \leq 3$) is a bounded domain with smooth boundary $\partial\Omega$; ν is the outward unit normal vector of the boundary $\partial\Omega$. The homogeneous Neumann boundary conditions indicate that the predator–prey system is self-contained with zero population flux across the boundary. The positive constants d_1, d_2 are diffusion coefficients, and the initial data $u_0(x), v_0(x)$ are non-negative continuous functions. r_1, K, c, m, r_2 , and h are positive constants.

By applying the following scaling to (2),

$$\begin{aligned} r_1 t &\mapsto t, & \frac{u}{K} &\mapsto u, & v &\mapsto v, \\ \frac{d_1}{r_1} &\mapsto d_1, & \frac{d_2}{r_1} &\mapsto d_2, & \frac{c}{Kr_1} &\mapsto \beta, \\ \frac{m}{K^2} &\mapsto m, & Kh &\mapsto \delta, & \frac{r_2}{r_1} &\mapsto r, \end{aligned}$$

it can be simplified as follows (for simplicity, taking $\delta = 1$),

$$\begin{cases} \frac{\partial u}{\partial t} - d_1 \Delta u = u(1 - u) - \frac{\beta u^2 v}{u^2 + mv^2}, & x \in \Omega, \quad t > 0, \\ \frac{\partial v}{\partial t} - d_2 \Delta v = rv \left(1 - \frac{v}{u}\right), & x \in \Omega, \quad t > 0, \\ \frac{\partial u}{\partial \nu} = \frac{\partial v}{\partial \nu} = 0, & x \in \partial\Omega, \quad t > 0, \\ u(x, 0) = u_0(x) \geq 0, & x \in \Omega, \\ v(x, 0) = v_0(x) \geq 0, & x \in \Omega. \end{cases} \quad (3)$$

The rest of this paper is organized as follows. In Sec. 2, we first consider the diffusion-driven instability of the positive equilibrium for R–D system (3) when the spatial domain is a bounded interval. In Sec. 3, we study the direction of Hopf bifurcation and the stability of the bifurcating periodic solution, which is a spatially homogeneous periodic solution of the R–D system (3). In Sec. 4, we present a detailed investigation of the Turing–Hopf bifurcation. The paper ends with a brief discussion in Sec. 5.

2. Turing Instability

We can see that system (3) has a unique constant positive steady-state solution $E^* = (u^*, v^*)$ under the condition $\beta < 1 + m$, where

$$(u^*, v^*) = \left(1 - \frac{\beta}{1 + m}, 1 - \frac{\beta}{1 + m}\right).$$

From the viewpoint of ecology, the existence of constant positive steady-state solutions implies the coexistence of both the prey and predators.

In this section, we will derive conditions for the Turing instability of the spatially homogeneous equilibrium (u^*, v^*) of the reaction–diffusion

predator–prey system (3). Here, we consider the special case with no-flux boundary conditions in a one-dimensional interval $(0, l)$:

$$\begin{cases} \frac{\partial u}{\partial t} - d_1 \Delta u = u(1 - u) - \frac{\beta u^2 v}{u^2 + mv^2}, \\ \qquad \qquad \qquad x \in (0, l), \quad t > 0, \\ \frac{\partial v}{\partial t} - d_2 \Delta v = rv \left(1 - \frac{v}{u}\right), \quad x \in (0, l), \quad t > 0, \\ \frac{\partial u}{\partial \nu} = \frac{\partial v}{\partial \nu} = 0, \quad x = 0, l, \quad t > 0, \\ u(x, 0) = u_0(x) \geq 0, \\ v(x, 0) = v_0(x) \geq 0, \end{cases} \quad x \in (0, l), \quad (4)$$

where $l > 0$ is the length of interval. While our calculations can be carried over to higher-dimensional spatial domains, we restrict ourselves to the case of spatial domain $(0, l)$, for which the structure of the

eigenvalues is clear. To this end, let

$$\begin{pmatrix} u \\ v \end{pmatrix} = \begin{pmatrix} \rho_1 \\ \rho_2 \end{pmatrix} \exp(\mu t + ikx),$$

where μ is the growth rate of perturbation in time t , ρ_1, ρ_2 are the amplitudes and k is the wave number of the solutions.

The linearized system of (4) at (u^*, v^*) has the form:

$$\begin{pmatrix} u_t \\ v_t \end{pmatrix} = L \begin{pmatrix} u \\ v \end{pmatrix} := D \begin{pmatrix} u_{xx} \\ v_{xx} \end{pmatrix} + J \begin{pmatrix} u \\ v \end{pmatrix}, \quad (5)$$

where the Jacobian matrix J is given by

$$J := \begin{pmatrix} r_0 & \sigma \\ r & -r \end{pmatrix} = \begin{pmatrix} \frac{2\beta - (1+m)^2}{(1+m)^2} & \frac{\beta(m-1)}{(1+m)^2} \\ r & -r \end{pmatrix}$$

and $D = \text{diag}(d_1, d_2)$. L is a linear operator with domain $D_L = X_C := X \oplus iX = \{x_1 + ix_2 : x_1, x_2 \in X\}$, where

$$X := \left\{ (u, v) \in H^2[(0, l)] \times H^2[(0, l)] \mid \begin{array}{l} u_x(0, t) = u_x(l, t) = 0 \\ v_x(0, t) = v_x(l, t) = 0 \end{array} \right\}$$

and $H^2[(0, l)]$ denotes the standard Sobolev space. Denote

$$J_k := J - k^2 D = \begin{pmatrix} r_0 - k^2 d_1 & \sigma \\ r & -r - k^2 d_2 \end{pmatrix}.$$

It is clear that the eigenvalues of the operator L are given by the eigenvalues of the matrix J_k . The characteristic equation of J_k is

$$P_k(\mu) := \mu^2 - \text{Tr} J_k \cdot \mu + \text{Det} J_k = 0, \quad (6)$$

where

$$\text{Tr} J_k := r_0 - r - k^2(d_1 + d_2), \quad (7)$$

$$\begin{aligned} \text{Det} J_k &:= d_1 d_2 k^4 + (rd_1 - r_0 d_2) k^2 \\ &\quad - r(r_0 + \sigma). \end{aligned} \quad (8)$$

We can check that

$$\begin{aligned} -r(r_0 + \sigma) &= \frac{-r[2\beta - (1+m)^2]}{(1+m)^2} - \frac{r\beta(m-1)}{(1+m)^2} \\ &= \frac{r(1+m-\beta)}{(1+m)^2} > 0. \end{aligned}$$

The roots of (6) yield the dispersion relation

$$\mu_k = \frac{\text{Tr} J_k \pm \sqrt{(\text{Tr} J_k)^2 - 4 \text{Det} J_k}}{2}.$$

If we assume that $2\beta < \lambda(1+m)^2$, then $r_0 < 0$. It is easy to see that $\text{Tr} J_k < 0$ and $\text{Det} J_k > 0$. Thus, we can conclude that the two roots of $P_k(\mu) = 0$ both have negative real parts for all $k \geq 0$. Therefore, we have the following result.

Proposition 2.1. *Assume that $\beta < \min\{1 + m, \frac{1}{2}(1+m)^2\}$. Then the unique positive constant steady state (u^*, v^*) of (4) is locally asymptotically stable.*

Remark 2.2. In Proposition 2.1, we supposed that $\beta < \min\{1 + m, \frac{1}{2}(1+m)^2\}$. If $m = 1$, then $1 + m = \frac{1}{2}(1+m)^2 = 2$; if $m < 1$, then $1 + m > \frac{1}{2}(1+m)^2$; if $m > 1$, then $1 + m < \frac{1}{2}(1+m)^2$.

Next, we investigate the Turing stability of the spatially homogeneous equilibrium (u^*, v^*) of R–D system (4). Turing condition is the one in which the uniform steady state of the reaction–diffusion equation is stable for the corresponding ordinary

differential equations, but it is unstable in the partial differential equations with diffusion terms. It is easy to see that the positive equilibrium (u^*, v^*) for the corresponding ordinary differential equations (i.e. $d_1 = d_2 = 0$) is locally asymptotically stable when $r > r_0$ and a family of small amplitude periodic solutions can bifurcate from the positive equilibrium (u^*, v^*) when r crosses through the critical value r_0 .

We shall restrict our discussion to $r_0 > 0$, i.e. $2\beta > (1 + m)^2$. In this case, $m < 1$ and thus $\sigma < 0$ (see Remark 2.2). It is well known that the positive equilibrium (u^*, v^*) of system (4) is unstable when (6) has at least one root with positive real part. Note that $\text{Tr } J_k < 0$ when $r > r_0$. Hence, (6) has no complex roots with positive real part. For the sake of convenience, define

$$\begin{aligned} \varphi(k^2) &:= \text{Det } J_k \\ &= d_1 d_2 k^4 + (rd_1 - r_0 d_2)k^2 - r(r_0 + \sigma), \end{aligned}$$

which is a quadratic polynomial with respect to k^2 . It is necessary to determine the sign of $\varphi(k^2)$. When $\varphi(k^2) < 0$, (6) has two real roots in which one is positive and another is negative. When

$$H(d_1, d_2) := rd_1 - r_0 d_2 < 0, \quad (9)$$

it is easy to obtain that $\varphi(k^2)$ will take the minimum value

$$\begin{aligned} \min_k \varphi(k^2) &= -r(r_0 + \sigma) - \frac{(rd_1 - r_0 d_2)^2}{4d_1 d_2} \\ &< 0 \end{aligned} \quad (10)$$

at $k^2 = k_{\min}^2$, where

$$k_{\min}^2 = -\frac{rd_1 - r_0 d_2}{2d_1 d_2}.$$

Define the ratio $\theta = d_2/d_1$ and let

$$\begin{aligned} \Lambda(d_1, d_2) &:= (rd_1 - r_0 d_2)^2 + 4r(r_0 + \sigma)d_1 d_2 \\ &= r_0^2 d_2^2 + 2r(r_0 + 2\sigma)d_1 d_2 + r^2 d_1^2. \end{aligned}$$

Then

$$\Lambda(d_1, d_2) = 0 \Leftrightarrow r_0^2 \theta^2 + 2r(r_0 + 2\sigma)\theta + r^2 = 0,$$

$$H(d_1, d_2) = 0 \Leftrightarrow \theta = \frac{r}{r_0} \equiv \theta^*.$$

Note that $-r(r_0 + \sigma) > 0$ and $\sigma < 0$, we have

$$4r^2(r_0 + 2\sigma)^2 - 4r^2 r_0^2 = 16r^2 \sigma(r_0 + \sigma) > 0.$$

Then $\Lambda(d_1, d_2) = 0$ has two positive real roots

$$\theta_1 = \frac{-r(r_0 + 2\sigma) + 2r\sqrt{\sigma(r_0 + \sigma)}}{r_0^2} \quad (11)$$

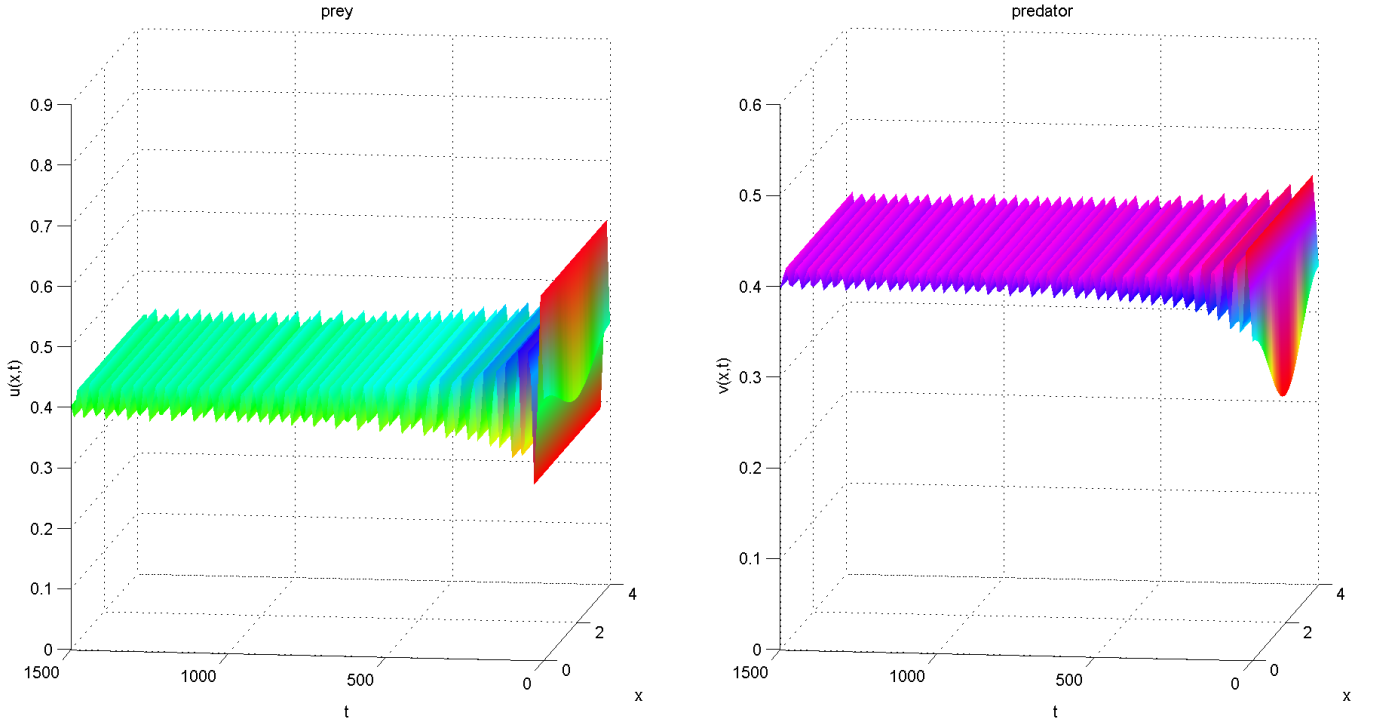


Fig. 1. Numerical simulations of the stable positive equilibrium solution for R–D system (14) with $r = 0.08 > r_0 = 0.0744$, $l = 4$, $(u_0(x), v_0(x)) = (0.4 + 0.03 \cos(\pi x/2), 0.3 + 0.05 \cos(\pi x/2))$, $d_1 = 1$ and $d_2 = 1$.

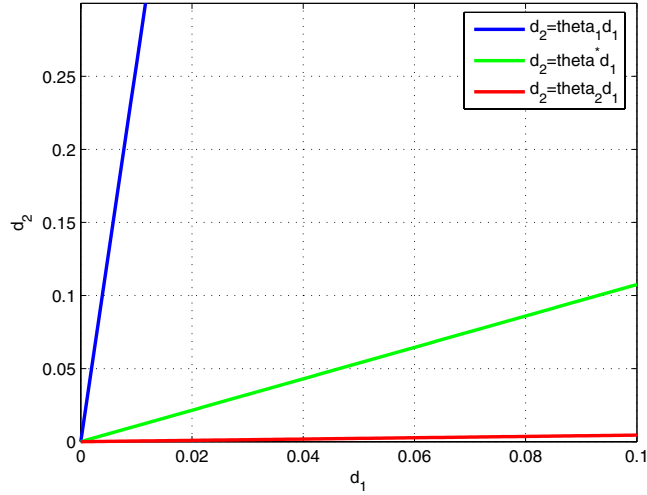


Fig. 2. Parameter space for Turing instability for R–D system (4) with $m = 0.1$, $\beta = 0.65$ and $r = 0.08$. The unstable region is the region between the line $d_2 = \theta_1 d_1$ and the d_2 -axis.

and

$$\theta_2 = \frac{-r(r_0 + 2\sigma) - 2r\sqrt{\sigma(r_0 + \sigma)}}{r_0^2}. \quad (12)$$

It is easy to find that $0 < \theta_2 < \theta^* < \theta_1$. Therefore, when $\frac{d_2}{d_1} > \theta_1$ holds, we have $\min_k \varphi(k^2) < 0$

and $H(d_1, d_2) < 0$, that is, if

$$d_2 > \frac{-rd_1(r_0 + 2\sigma) + 2rd_1\sqrt{\sigma(r_0 + \sigma)}}{r_0^2} \triangleq D_2, \quad (13)$$

then (u^*, v^*) is unstable. This indicates that Turing instability occurs.

Based on the above argument, we have the following result about diffusion-driven instability.

Theorem 2.3. Assume that $\beta < 1 + m$, $2\beta > (1 + m)^2$ and $r > r_0$. Then (u^*, v^*) is unstable for R–D system (4), that is, Turing instability occurs if $d_2 > D_2$, where D_2 is given in (13).

Remark 2.4. We can see that $\frac{d_2}{d_1} > 1$ under the assumption that $r > r_0$. Hence, for diffusive instability of system (4), the predators must diffuse faster than the prey. When cross-diffusion or anomalous diffusion is incorporated into the model, the restriction on the choice of the diffusion coefficients for Turing instability to happen may be lightened, see e.g. [Gambino et al., 2014; Vanag & Epstein, 2009], etc.

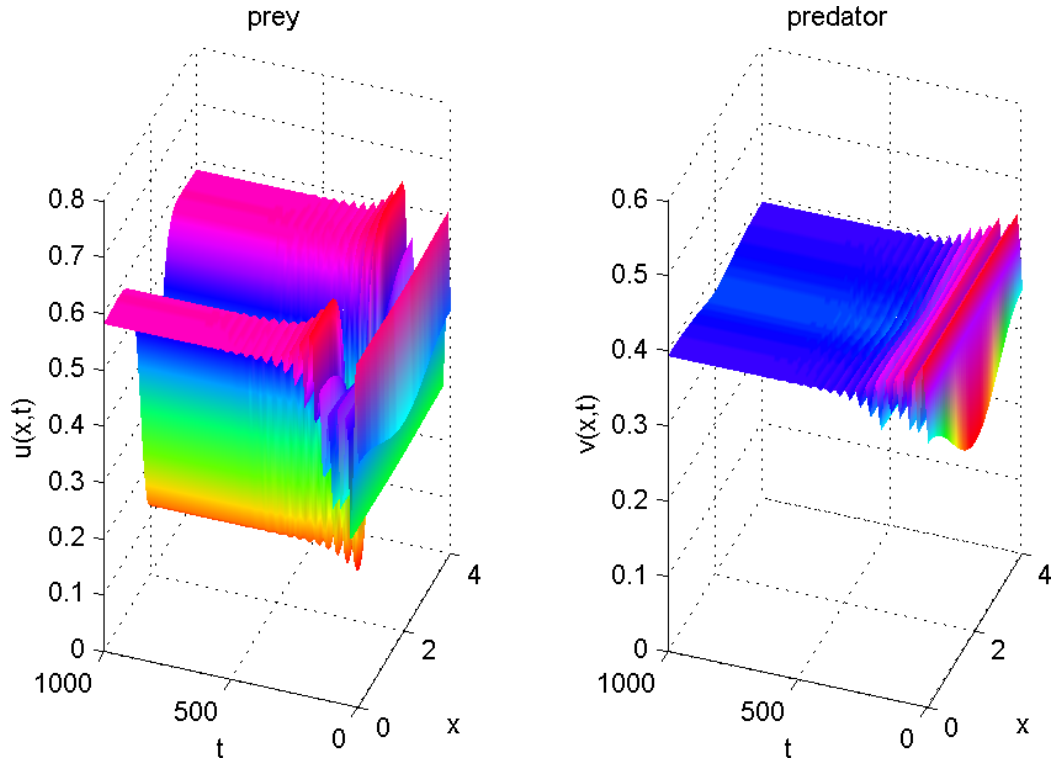


Fig. 3. Numerical simulations of the Turing instability for R–D system (14) with $r = 0.08 > r_0 = 0.0744$, $l = 4$, $(u_0(x), v_0(x)) = (0.4 + 0.03 \cos(\pi x/2), 0.3 + 0.05 \cos(\pi x/2))$, $d_1 = 0.008$ and $d_2 = 1$.

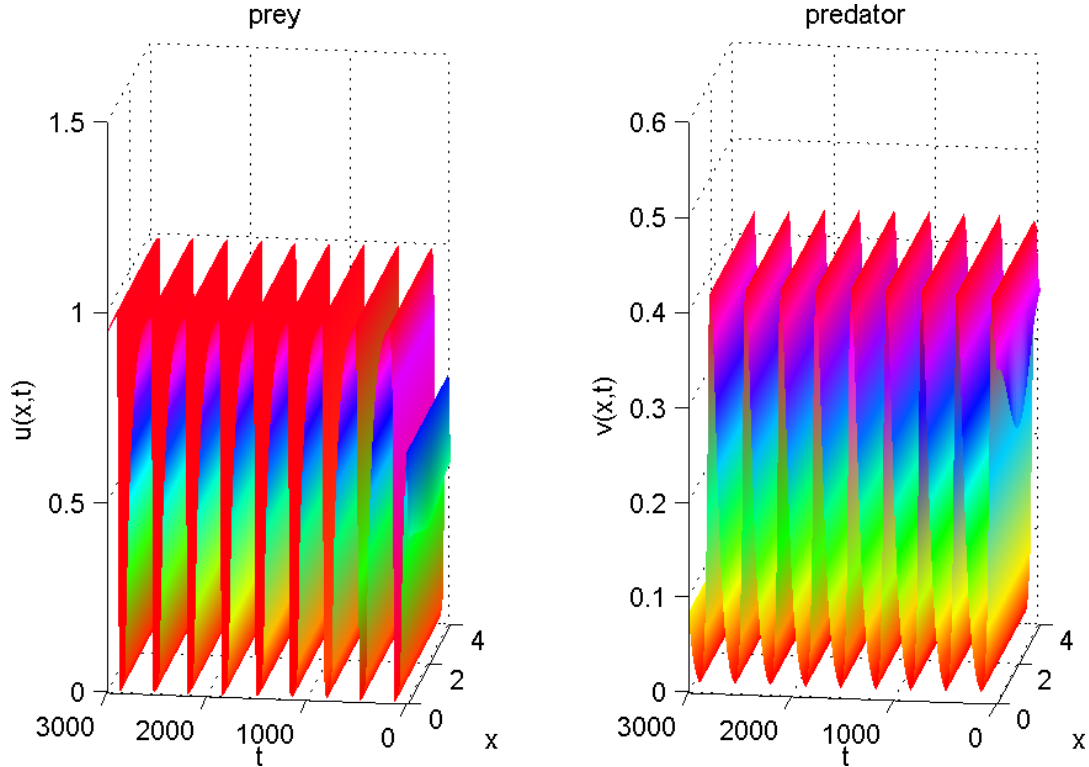


Fig. 4. Numerical simulations of the stable time periodic solutions for R–D system (14) with $r = 0.02 < r_0 = 0.0744$, $l = 4$, $(u_0(x), v_0(x)) = (0.4 + 0.03 \cos(\pi x/2), 0.3 + 0.05 \cos(\pi x/2))$, $d_1 = 1$ and $d_2 = 1$.

(spatially homogeneous) periodic solutions are orbitally asymptotically stable if $\text{Re}(c_1(r_0)) < 0$; the direction of the Hopf bifurcation is supercritical and the bifurcating periodic solutions are unstable if $\text{Re}(c_1(r_0)) > 0$.

Remark 3.2. In Theorem 3.1, we require that $\beta < 1 + m$ and $2\beta > (1 + m)^2$ hold simultaneously. In this case, we need the inequality $1 + m > \frac{1}{2}(1 + m)^2$ to hold, i.e. $m < 1$, and thus $\sigma < 0$.

Example 3.3. To perform some numerical simulations on Hopf bifurcation, we continue to consider the R–D system (14). We knew that when $r = 0.08 > r_0 = 0.0744$ and $d_2/d_1 < \theta_1$, the positive equilibrium E^* is locally asymptotically stable (Fig. 1). By Theorem 3.1, Hopf bifurcation occurs at $r = r_0$ and the bifurcating periodic solutions exist when $r < r_0$. Choosing $r = 0.02 < 0.0744$, we have $\text{Re}(c_1(r_0)) = -0.9927 < 0$, which indicates that the bifurcating periodic solutions are orbitally asymptotically stable (see Fig. 4).

4. Turing–Hopf Bifurcation

Ecologically speaking, the Turing instability breaks the spatial symmetry leading to the pattern

formation that is stationary in time and oscillatory in space, while the Hopf bifurcation breaks the temporal symmetry of the system and gives rise to oscillations which are uniform in space and periodic in time. In this part, we will investigate the coupling between these two different instabilities, i.e. Turing–Hopf bifurcation, in the (r, d_1) parameter space.

Assume that $\beta < 1 + m$ and $2\beta > (1 + m)^2$. Thus, $-(r_0 + \sigma) > 0$ and $\sigma < 0$. We choose r as the bifurcation parameter. From Theorem 3.1, we know that the critical value of Hopf bifurcation parameter r is

$$r^H = r_0 = \frac{2\beta - (1 + m)^2}{(1 + m)^2}.$$

At the bifurcation point, the frequency of these temporal oscillations is given by

$$\begin{aligned} \omega_H &= \text{Im}(\mu_k) = \sqrt{\text{Det } J_k|_{k=0}} \\ &= \sqrt{-r(r_0 + \sigma)}. \end{aligned}$$

Based on the analysis in Sec. 2, we know that the Turing instability occurs when $d_1 \ll d_2$. In the

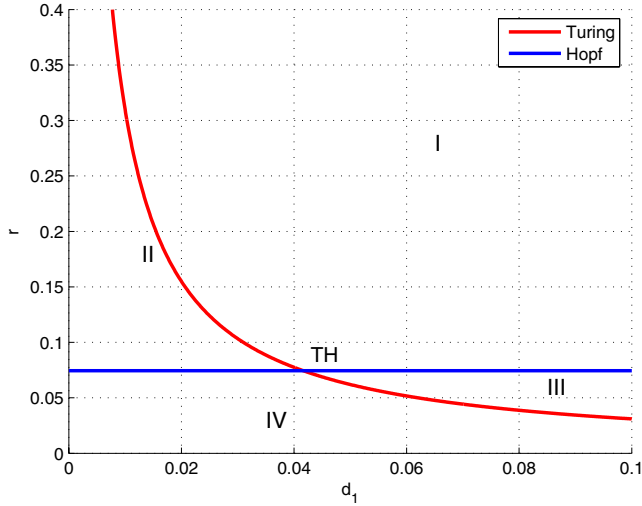


Fig. 5. Turing–Hopf bifurcation diagram for R–D system (4) with $m = 0.1$, $\beta = 0.65$ and $d_2 = 1$.

following, we fix $d_2 = 1$. From (11), the critical value of Turing bifurcation parameter r takes the form,

$$r^T = \frac{1}{d_1} \left(\frac{r_0}{\sqrt{-\sigma} + \sqrt{-(r_0 + \sigma)}} \right)^2.$$

At the Turing instability threshold, the bifurcation of stationary spatially periodic patterns is

characterized by the wavenumber k_T with

$$k_T = \sqrt{\frac{-r(r_0 + \sigma)}{d_1}}.$$

In Fig. 5, the curves at which Hopf and Turing instabilities occur are plotted in the (r, d_1) parameter space for fixed $m = 0.1$, $\beta = 0.65$ and $d_2 = 1$. The Hopf bifurcation curve and the Turing instability curve divide the parametric space into four distinct regions. In region I, the upper part of the displayed parameter space, the positive equilibrium is the only stable solution of R–D system (4). Region II is the region of pure Turing bifurcation, while region III is the region of pure Hopf bifurcation. In region IV, located below the two bifurcation curves, both Turing and Hopf bifurcations occur. This can give rise to an interaction of both types of bifurcations, producing particularly complex spatiotemporal patterns if the thresholds for both instabilities occur close to each other. This is the case in the neighborhood of a degenerate point (marked by TH), where the Turing and the Hopf bifurcations coincide: it is called a codimension-two Turing–Hopf point, since the two control variables are necessary to fix these bifurcation points in a generic system of equations.

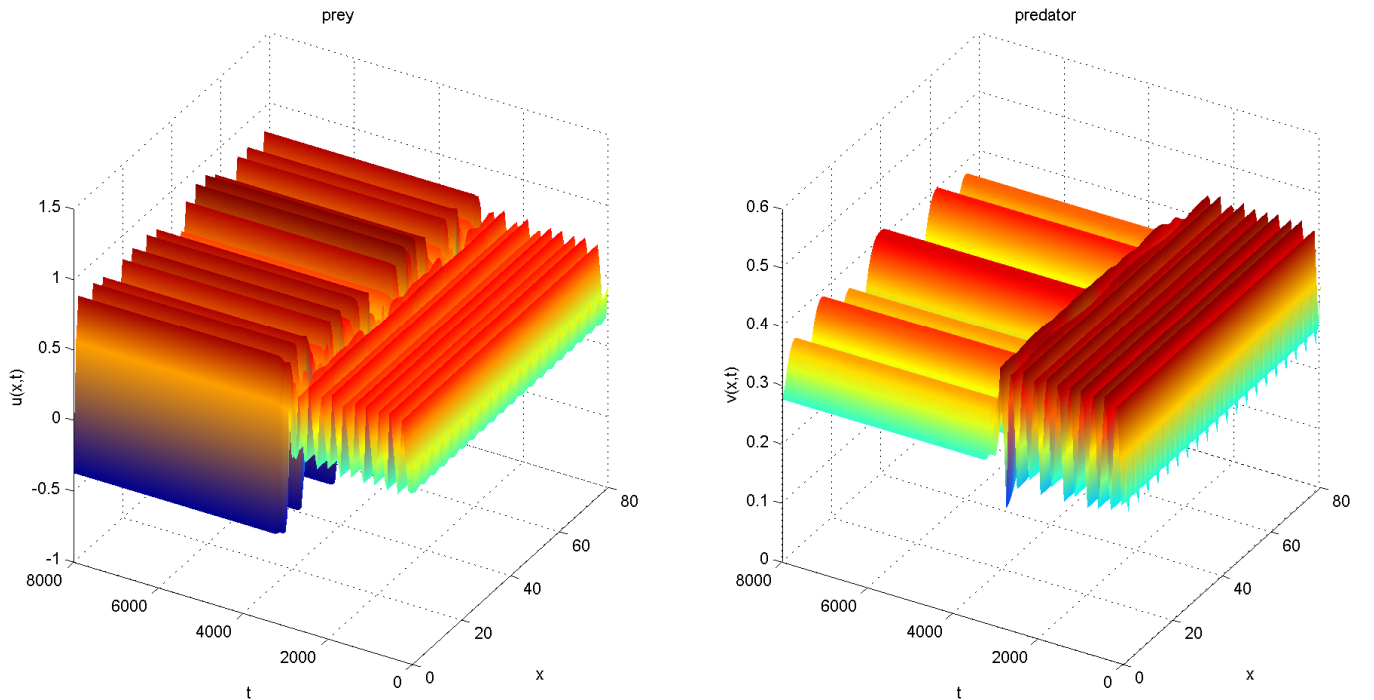


Fig. 6. Numerical simulations of the spatiotemporal Turing–Hopf structures for R–D system (14) with $r = 0.05 < r_0 = 0.0744$, $l = 80$, $(u_0(x), v_0(x)) = (0.4 + 0.03 \cos(\pi x/2), 0.3 + 0.05 \cos(\pi x/2))$, $d_1 = 0.005$ and $d_2 = 1$.

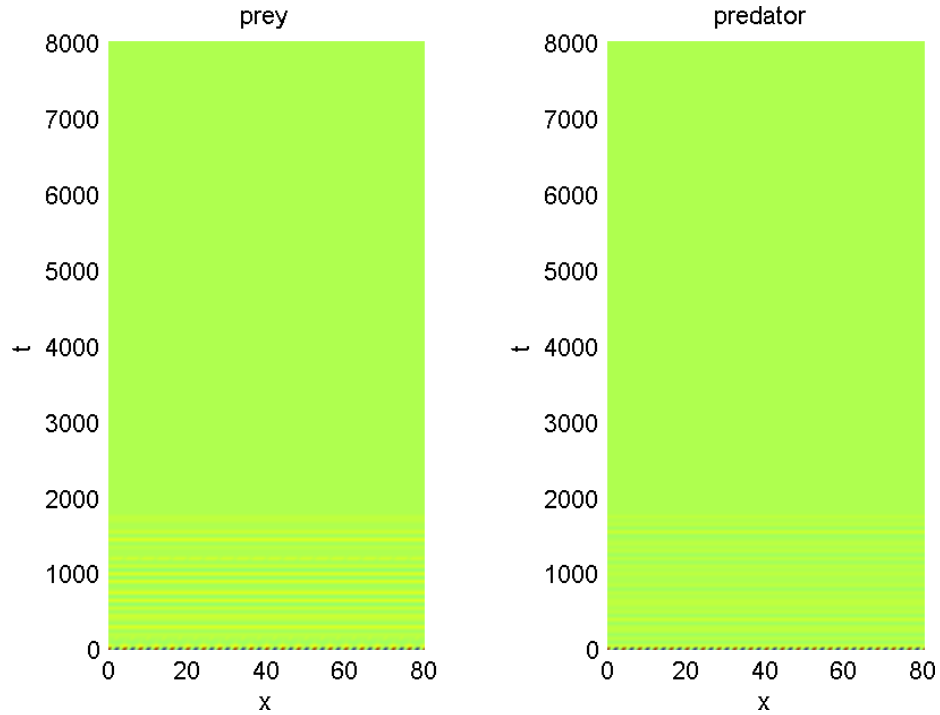


Fig. 7. Numerical simulations of the uniformly convergent solutions of R-D system (14) in the (x, t) plane with $r = 0.1 > r_0 = 0.0744$, $l = 80$, $(u_0(x), v_0(x)) = (0.4 + 0.1 \cos(\pi x/2), 0.4 + 0.1 \cos(\pi x/2))$, $d_1 = 0.04$ and $d_2 = 1$.

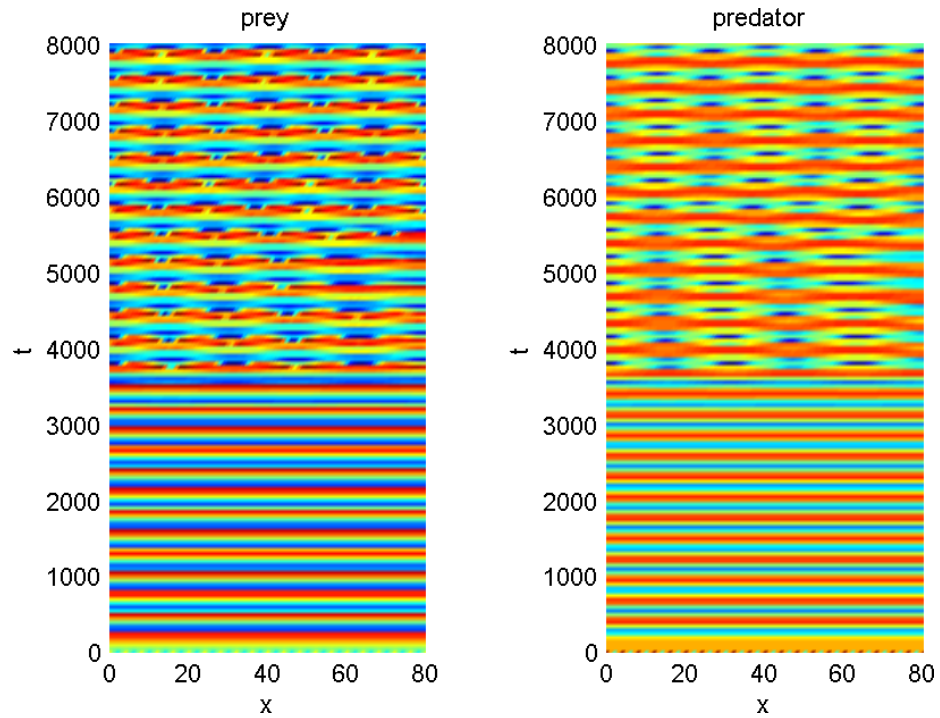


Fig. 8. Numerical simulations of the spatially inhomogeneous time periodic solutions of R-D system (14) in the (x, t) plane with $r = 0.05 < r_0 = 0.0744$, $l = 80$, $(u_0(x), v_0(x)) = (0.4 + 0.1 \cos(\pi x/2), 0.4 + 0.1 \cos(\pi x/2))$, $d_1 = 0.04$ and $d_2 = 1$.

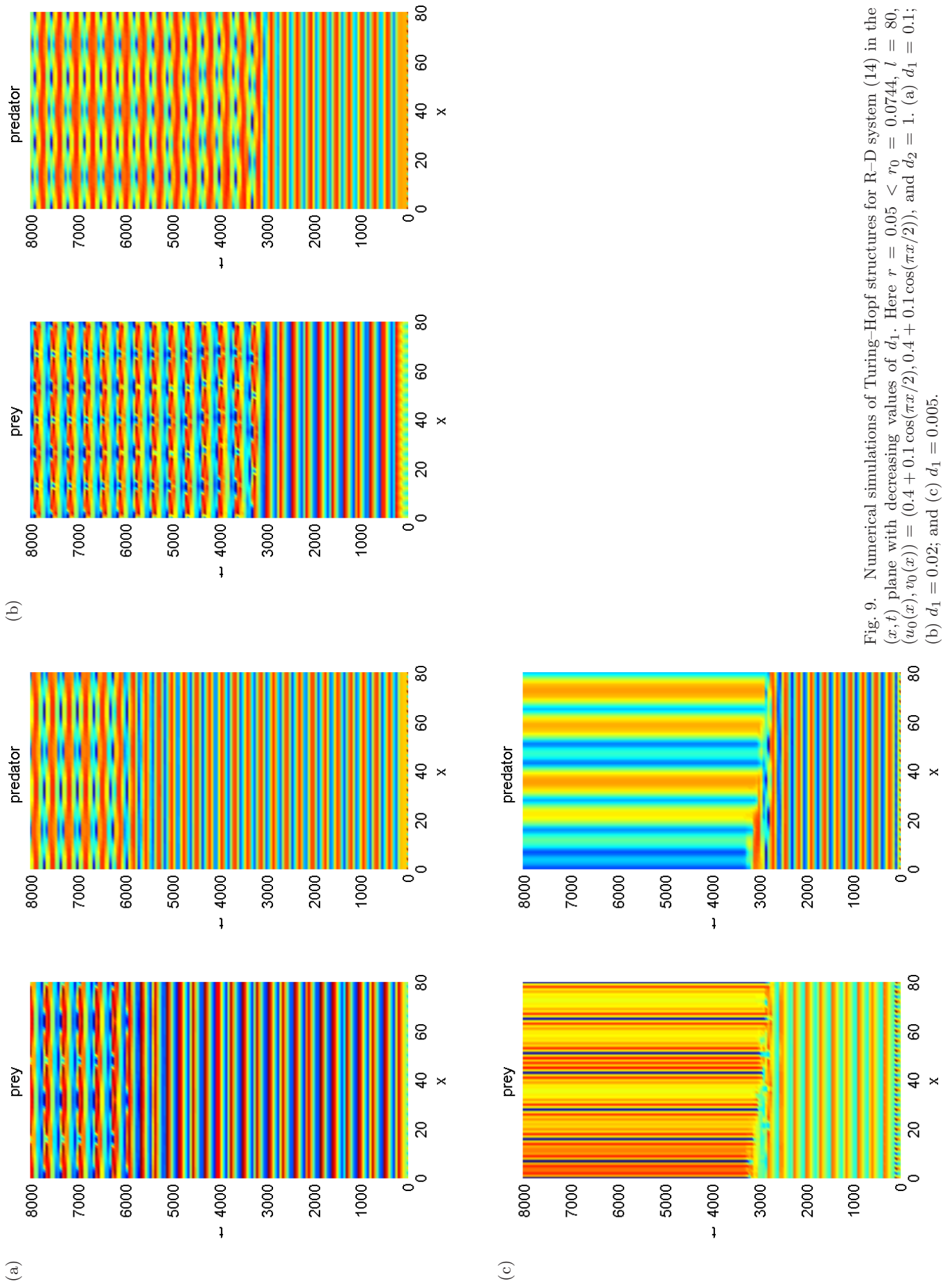


Fig. 9. Numerical simulations of Turing-Hopf structures for R-D system (14) in the (x, t) plane with decreasing values of d_1 . Here $r = 0.05 < r_0 = 0.0744$, $l = 80$, $(u_0(x), v_0(x)) = (0.4 + 0.1 \cos(\pi x/2), 0.4 + 0.1 \cos(\pi x/2))$, and $d_2 = 1$. (a) $d_1 = 0.1$; (b) $d_1 = 0.02$; and (c) $d_1 = 0.005$.

At the Turing–Hopf point, we have $r^H = r^T$; in other words,

$$r_0 = \frac{1}{d_1} \left(\frac{r_0}{\sqrt{-\sigma} + \sqrt{-(r_0 + \sigma)}} \right)^2.$$

This condition is satisfied for the critical value of d_1 :

$$d_1^* = \frac{r_0}{(\sqrt{-\sigma} + \sqrt{-(r_0 + \sigma)})^2}.$$

If $d_1 < d_1^*$, then $r^H < r^T$. With increasing r , the Hopf threshold is the first to be crossed and thus the Hopf bifurcation will be the first to occur near the criticality. On the contrary, if $d_1 > d_1^*$, the first bifurcation will occur toward Turing pattern.

Example 4.1. Once again consider, as an example, R–D system (14). Figure 6 gives the Turing–Hopf structures for the system.

Remark 4.2. We provide more numerical simulations in the (x, t) plane to see how the pattern forms strictly depend on the two instability mechanisms — one occurs between the two instabilities. From Fig. 5, we know that neither Turing nor Hopf bifurcation occurs when $d_1 = 0.04$ and $r = 0.1$. In such a situation, solutions approach the steady state uniformly in space (see Fig. 7). When r is decreased to 0.05, both Turing and Hopf bifurcations occur. Figure 8 provides a spatially inhomogeneous time periodic solution. Finally, when $r = 0.05$ is fixed, choose $d_1 = 0.1$, $d_1 = 0.02$ and $d_1 = 0.005$, respectively, Fig. 4 shows that the Turing effect is stronger when d_1 is smaller.

5. Discussion

In this paper, we have considered a diffusive Leslie predator–prey system with ratio-dependent Holling type III functional response under homogeneous Neumann boundary conditions. For the reaction–diffusion model, we first investigated Turing instability which induces spatially inhomogeneous solutions. Next, we performed a detailed Hopf bifurcation analysis of the model and derived conditions to determine the direction of Hopf bifurcation and stability of the bifurcating temporal periodic solutions by applying the normal form theory and the center manifold reduction. Then we showed that at the intersecting points of the Turing

bifurcation and Hopf bifurcations curves, the model exhibits Turing–Hopf bifurcation, which produces spatiotemporal patterns for the reaction–diffusion predator–prey system.

The positive equilibrium and periodic solutions of the local system are spatially homogeneous solutions of the diffusive system (4). Therefore, we can regard the dynamics of ODE model (i.e. $d_1 = d_2 = 0$) as subdynamics of the PDE model (4). Moreover, the direction of Hopf bifurcation for system (4) at $r = r_0$ is the same as that of ODE system. However, the stability of the positive equilibrium (u^*, v^*) can change due to the effect of diffusion.

It is well known that predator–prey models with ratio-dependent Holling type II functional response have very rich and complex dynamical behaviors (see [Hsu et al., 2001; Kuang, 1999; Kuang & Beretta, 1998; Li & Kuang, 2007; Liang & Pan, 2007; Ruan et al., 2008, 2010; Xiao & Ruan, 2001]). If both the predators and their prey can disperse randomly in their habits but do not cross the boundary, our results demonstrate that the diffusive Leslie–Gower predator–prey system with ratio-dependent Holling type III functional response can exhibit spatial patterns (via Turing instability), temporal patterns (via Hopf bifurcation), as well as spatiotemporal patterns (via Turing–Hopf bifurcation).

Acknowledgments

Part of this work was performed when the first author was visiting the University of Miami in 2013, he would like to thank the faculty and staff in the Department of Mathematics at the University of Miami for their warm hospitality. The authors also thank the referees for their valuable comments which have led to a much improved paper.

References

- Arditi, R. & Ginzburg, L. R. [1989] “Coupling in predator–prey dynamics: Ratio-dependence,” *J. Theoret. Biol.* **139**, 311–326.
- Arditi, R., Ginzburg, L. R. & Akcakaya, H. R. [1991] “Variation in plankton densities among lakes: A case for ratio-dependent models,” *Amer. Nat.* **138**, 1287–1296.
- Arditi, R. & Saiah, H. [1992] “Empirical evidence of the role of heterogeneity in ratio-dependent consumption,” *Ecology* **73**, 1544–1551.

- Baurmann, M., Gross, T. & Feudela, U. [2007] “Instabilities in spatially extended predator–prey systems: Spatio-temporal patterns in the neighborhood of Turing–Hopf bifurcations,” *J. Theoret. Biol.* **245**, 220–229.
- Bazykin, A. D. [1998] *Nonlinear Dynamics of Interacting Populations*, World Sci. Ser. Nonlinear Sci. Ser. A, Vol. 11 (World Scientific, Singapore).
- Camara, B. I. & Aziz-Alaoui, M. A. [2009] “Turing and Hopf patterns formation in a predator–prey model with Leslie–Gower-type functional response,” *Dyn. Cont. Discr. Impuls. Syst. Ser. B* **16**, 479–488.
- Collings, J. B. [1997] “The effects of the functional response on the behavior of a mite predator–prey interaction model,” *J. Math. Biol.* **36**, 149–168.
- Du, Y., Peng, R. & Wang, M. [2009] “Effect of a protection zone in the diffusive Leslie predator–prey model,” *J. Diff. Eqs.* **246**, 3932–3956.
- Freedman, H. I. & Mathsen, R. M. [1993] “Persistence in predator–prey systems with ratio-dependent predator influence,” *Bull. Math. Biol.* **55**, 817–827.
- Gambino, G., Lombardo, M. C., Sammartino, M. & Sciacca, V. [2013] “Turing pattern formation in the Brusselator model with nonlinear diffusion,” *Phys. Rev. E* **88**, 042925.
- Gambino, G., Lombardo, M. C. & Sammartino, M. [2014] “Turing instability and pattern formation for the Lengyel–Epstein system with nonlinear diffusion,” *Acta Appl. Math.* **132**, 283–294.
- Golovin, A., Matkowsky, B. & Volpert, V. [2008] “Turing pattern formation in the Brusselator model with superdiffusion,” *SIAM J. Appl. Math.* **69**, 251–272.
- Hassard, B. D., Kazarinoff, N. D. & Wan, Y.-H. [1981] *Theory and Applications of Hopf Bifurcation* (Cambridge University Press, Cambridge).
- Holling, C. S. [1965] “The functional response of predator to prey density and its role in mimicry and population regulation,” *Mem. Entomol. Soc. Can.* **97**, 5–60.
- Hsu, S.-B. & Huang, T.-W. [1995] “Global stability for a class of predator–prey systems,” *SIAM J. Appl. Math.* **55**, 763–783.
- Hsu, S.-B., Huang, T.-W. & Kuang, Y. [2001] “Rich dynamics of a ratio-dependent one-prey two-predators model,” *J. Math. Biol.* **43**, 377–396.
- Kuang, Y. & Beretta, E. [1998] “Global qualitative analysis of a ratio-dependent predator–prey system,” *J. Math. Biol.* **36**, 389–406.
- Kuang, Y. [1999] “Rich dynamics of Gause-type ratio-dependent predator–prey system,” *Fields Instit. Commun.* **21**, 325–337.
- Leslie, P. H. [1948] “Some further notes on the use of matrices in population mathematics,” *Biometrika* **35**, 213–245.
- Leslie, P. H. & Gower, J. C. [1960] “The properties of a stochastic model for the predator–prey type of interaction between two species,” *Biometrika* **47**, 219–234.
- Levin, S. A. & Segel, L. A. [1985] “Pattern generation in space and aspect,” *SIAM Rev.* **27**, 45–67.
- Li, B. & Kuang, Y. [2007] “Heteroclinic bifurcation in the Michaelis–Menten-type ratio-dependent predator–prey system,” *SIAM J. Appl. Math.* **67**, 1453–1464.
- Li, Y. & Xiao, D. [2007] “Bifurcations of a predator–prey system of Holling and Leslie types,” *Chaos Solit. Fract.* **34**, 606–620.
- Li, X., Jiang, W. & Shi, J. [2013] “Hopf bifurcation and Turing instability in the reaction–diffusion Holling–Tanner predator–prey model,” *IMA J. Appl. Math.* **78**, 287–306.
- Liang, Z. & Pan, H. [2007] “Qualitative analysis of a ratio-dependent Holling–Tanner model,” *J. Math. Anal. Appl.* **334**, 954–964.
- Malchow, H., Petrovskii, S. V. & Venturino, E. [2008] *Spatiotemporal Patterns in Ecology and Epidemiology: Theory, Models, and Simulation* (Chapman & Hall/CRC, Boca Raton).
- May, R. [1973] *Stability and Complexity in Model Ecosystems* (Princeton University Press, Princeton, NJ).
- Meixner, M., Wit, A. D., Bose, S. & Scholl, E. [1997] “Generic spatiotemporal dynamics near codimension-two Turing–Hopf bifurcations,” *Phys. Rev. E* **55**, 6690–6697.
- Murray, J. D. [1989] *Mathematical Biology* (Springer-Verlag, Berlin).
- Okubo, A. [1980] *Diffusion and Ecological Problems: Mathematical Models* (Springer-Verlag, Berlin).
- Peng, R. & Wang, M. [2008] “Qualitative analysis on a diffusive prey-predator model with ratio-dependent functional response,” *Sci. China Ser. A: Math.* **51**, 2043–2058.
- Peng, R. [2013] “Qualitative analysis on a diffusive and ratio-dependent predator–prey model,” *IMA J. Appl. Math.* **78**, 566–586.
- Ruan, S. [1998] “Diffusion-driven instability in the Gierer–Meinhardt model of morphogenesis,” *Nat. Res. Model.* **11**, 131–142.
- Ruan, S., Tang, Y. & Zhang, W. [2008] “Computing the heteroclinic bifurcation curves in predator–prey systems with ratio-dependent functional response,” *J. Math. Biol.* **57**, 223–241.
- Ruan, S., Tang, Y. & Zhang, W. [2010] “Versal unfoldings of predator–prey systems with ratio-dependent functional response,” *J. Diff. Eqs.* **249**, 1410–1435.
- Smith, J. M. [1974] *Models in Ecology* (Cambridge University Press, Cambridge).

- Turing, A. [1952] “The chemical basis of morphogenesis,” *Philos. Trans. Roy. Soc. Lond. Ser. B* **237**, 37–72.
- Tzou, J. C., Bayliss, A., Matkowsky, B. J. & Volpert, V. A. [2011] “Interaction of Turing and Hopf modes in the superdiffusive Brusselator model near a codimension two bifurcation point,” *Math. Model. Nat. Phenom.* **6**, 87–118.
- Tzou, J. C., Ma, Y.-P., Bayliss, A., Matkowsky, B. J. & Volpert, V. A. [2013] “Homoclinic snaking near a codimension-two Turing–Hopf bifurcation point in the Brusselator model,” *Phys. Rev. E* **87**, 022908.
- Vanag, V. K. & Epstein, I. R. [2009] “Cross-diffusion and pattern formation in reaction–diffusion systems,” *Phys. Chem. Chem. Phys.* **11**, 897–912.
- Wang, W., Liu, Q.-X. & Jin, Z. [2007] “Spatiotemporal complexity of a ratio-dependent predator–prey system,” *Phys. Rev. E* **75**, 051913.
- Wang, M. [2008] “Stability and Hopf bifurcation for a prey-predator model with prey-stage structure and diffusion,” *Math. Biosci.* **212**, 149–160.
- Wit, A. D., Lima, D., Dewel, G. & Borckmans, P. [1996] “Spatiotemporal dynamics near a codimension-two point,” *Phys. Rev. E* **54**, 261–271.
- Xiao, D. & Ruan, S. [2001] “Global dynamics of a ratio-dependent predator–prey system,” *J. Math. Biol.* **43**, 268–290.
- Yi, F., Wei, J. & Shi, J. [2009] “Bifurcation and spatiotemporal patterns in a homogeneous diffusive predator–prey system,” *J. Diff. Eqs.* **246**, 1944–1977.
- Zhang, J.-F., Li, W.-T. & Wang, Y.-X. [2011] “Turing patterns of a strongly coupled predator–prey system with diffusion effects,” *Nonlin. Anal.* **74**, 847–858.

Appendix: Calculation of $\text{Re}(c_1(r_0))$

In the Appendix, following the techniques and procedure in [Hassard *et al.*, 1981] we give the expression of $\text{Re}(c_1(r_0))$, which is used to determine the direction of the Hopf bifurcation and stability of bifurcating periodic solutions. Let L^* be the conjugate operator of L defined as (5):

$$L^* \begin{pmatrix} u \\ v \end{pmatrix} := D \begin{pmatrix} u_{xx} \\ v_{xx} \end{pmatrix} + J^* \begin{pmatrix} u \\ v \end{pmatrix}, \quad (\text{A.1})$$

where

$$J^* := J^T = \begin{pmatrix} \frac{2\beta - (1+m)^2}{(1+m)^2} & r \\ \frac{m-1}{(1+m)^2} & -r \end{pmatrix},$$

with the domain $D_{L^*} = X_C$. Let

$$q := \begin{pmatrix} q_1 \\ q_2 \end{pmatrix} = \begin{pmatrix} 1 \\ -\frac{r_0}{\sigma} + \frac{\omega_0}{\sigma}i \end{pmatrix},$$

$$q^* := \begin{pmatrix} q_1^* \\ q_2^* \end{pmatrix} = \frac{\sigma}{2\pi\omega_0} \begin{pmatrix} \frac{\omega_0}{\sigma} + \frac{r_0}{\sigma}i \\ i \end{pmatrix}.$$

For any $a \in D_{L^*}$, $b \in D_L$, it is not difficult to verify that

$$\langle L^*a, b \rangle = \langle a, Lb \rangle, \quad L(r_0)q = i\omega_0q,$$

$$L^*(r_0)q^* = -i\omega_0q^*, \quad \langle q^*, q \rangle = 1, \quad \langle q^*, \bar{q} \rangle = 0,$$

where $\langle a, b \rangle = \int_0^\pi \bar{a}^T b \, dx$ denotes the inner product in $L^2[(0, l)] \times L^2[(0, l)]$.

Following Hassard *et al.* [1981], we decompose $X = X^C \oplus X^S$ with $X^C = \{zq + \bar{z}\bar{q} : z \in \mathbb{C}\}$, $X^S = \{w \in X : \langle q^*, w \rangle = 0\}$. For any $(u, v) \in X$, there exists $z \in \mathbb{C}$ and $w = (w_1, w_2) \in X^S$ such that $(u, v)^T = zq + \bar{z}\bar{q} + (w_1, w_2)^T$, $z = \langle q^*, (u, v)^T \rangle$. Thus,

$$\begin{cases} u = z + \bar{z} + w_1, \\ v = z \left(\frac{-r_0}{\sigma} + i\frac{\omega_0}{\sigma} \right) + \bar{z} \left(\frac{-r_0}{\sigma} - i\frac{\omega_0}{\sigma} \right) + w_2. \end{cases}$$

System (4) is reduced to the following system in the (z, w) -coordinates:

$$\begin{cases} \frac{dz}{dt} = i\omega_0z + \langle q^*, \tilde{f} \rangle, \\ \frac{dw}{dt} = Lw + H(z, \bar{z}, w), \end{cases} \quad (\text{A.2})$$

where

$$H(z, \bar{z}, w) = \tilde{f} - \langle q^*, \tilde{f} \rangle q - \langle \bar{q}^*, \tilde{f} \rangle \bar{q}$$

and $\tilde{f} = (f^1, f^2)^T$ [f^1 and f^2 are defined as (16)]. It is easy to obtain that

$$\langle q^*, \tilde{f} \rangle = \frac{1}{2\omega_0} [\omega_0 f^1 - i(r_0 f^1 + \sigma f^2)],$$

$$\langle \bar{q}^*, \tilde{f} \rangle = \frac{1}{2\omega_0} [\omega_0 f^1 + i(r_0 f^1 + \sigma f^2)],$$

$$\langle q^*, \tilde{f} \rangle q = \frac{1}{2\omega_0} \begin{pmatrix} \omega_0 f^1 - i(r_0 f^1 + \sigma f^2) \\ \omega_0 f^2 + i \left(\frac{\omega_0^2}{\sigma} f^1 + \frac{r_0^2}{\sigma} f^1 + r_0 f^2 \right) \end{pmatrix},$$

$$\langle \bar{q}^*, \tilde{f} \rangle \bar{q} = \frac{1}{2\omega_0} \begin{pmatrix} \omega_0 f^1 + i(r_0 f^1 + \sigma f^2) \\ \omega_0 f^2 - i\left(\frac{\omega_0^2}{\sigma} f^1 + \frac{r_0^2}{\sigma} f^1 + r_0 f^2\right) \end{pmatrix}.$$

Furthermore, we have $H(z, \bar{z}, w) = (0, 0)^T$. Let

$$H = \frac{H_{20}}{2} z^2 + H_{11} z \bar{z} + \frac{H_{02}}{2} \bar{z}^2 + o(|z|^3).$$

It follows from Appendix A of [Hassard *et al.*, 1981] that system (A.2) possesses a center manifold, and we can write w in the form:

$$w = \frac{w_{20}}{2} z^2 + w_{11} z \bar{z} + \frac{w_{02}}{2} \bar{z}^2 + o(|z|^3).$$

Thus, we have

$$\begin{cases} w_{20} = (2i\omega_0 I - L)^{-1} H_{20}, \\ w_{11} = (-L)^{-1} H_{11}, \\ w_{02} = \bar{w}_{20}. \end{cases}$$

This implies that $w_{20} = w_{02} = w_{11} = 0$. For later uses, denote

$$\begin{aligned} \sigma_1 &:= f_{uu}^1 q_1^2 + 2f_{uv}^1 q_1 q_2 + f_{vv}^1 q_2^2 \\ &= 2A_{20} + 2A_{11} q_2, \\ \sigma_2 &:= f_{uu}^2 q_1^2 + 2f_{uv}^2 q_1 q_2 + f_{vv}^2 q_2^2 \\ &= 2B_{20} + 2B_{11} q_2 + 2B_{02} q_2^2, \end{aligned}$$

$$\begin{aligned} \nu_1 &:= f_{uu}^1 |q_1|^2 + f_{uv}^1 (q_1 \bar{q}_2 + \bar{q}_1 q_2) + f_{vv}^1 |q_2|^2 \\ &= 2A_{20} + A_{11} (q_2 + \bar{q}_2), \\ \nu_2 &:= f_{uu}^2 |q_1|^2 + f_{uv}^2 (q_1 \bar{q}_2 + \bar{q}_1 q_2) + f_{vv}^2 |q_2|^2 \\ &= 2B_{20} + B_{11} (q_2 + \bar{q}_2) + 2B_{02} |q_2|^2, \\ \tau_1 &:= f_{uuu}^1 |q_1|^2 q_1 + f_{uuv}^1 (2|q_1|^2 q_2 + q_1^2 \bar{q}_2) \\ &\quad + f_{uvv}^1 (2q_1 |q_2|^2 + \bar{q}_1 q_2^2) + f_{vvv}^1 |q_2|^2 q_2, \\ &= 6A_{30} + 2A_{21} (2q_2 + \bar{q}_2), \\ \tau_2 &:= f_{uuu}^2 |q_1|^2 q_1 + f_{uuv}^2 (2|q_1|^2 q_2 + q_1^2 \bar{q}_2) \\ &\quad + f_{uvv}^2 (2q_1 |q_2|^2 + \bar{q}_1 q_2^2) + f_{vvv}^2 |q_2|^2 q_2 \\ &= 6B_{30} + 2B_{21} (2q_2 + \bar{q}_2) + 2B_{12} (2|q_2|^2 + q_2^2), \end{aligned}$$

where all the partial derivatives evaluated at the point $(u, v, r) = (0, 0, r_0)$. Therefore, the reaction–diffusion system restricted to the center manifold in z, \bar{z} coordinates is given by

$$\begin{aligned} \frac{dz}{dt} &= i\omega_0 z + \frac{1}{2} g_{20} z^2 + g_{11} z \bar{z} + \frac{1}{2} g_{02} \bar{z}^2 \\ &\quad + \frac{1}{2} g_{21} z^2 \bar{z} + o(|z|^4), \end{aligned}$$

where $g_{20} = \langle q^*, (\sigma_1, \sigma_2)^T \rangle$, $g_{11} = \langle q^*, (\nu_1, \nu_2)^T \rangle$, $g_{21} = \langle q^*, (\tau_1, \tau_2)^T \rangle$. Note that $B_{02} = B_{20}$, $B_{11} = -2B_{20}$, $B_{21} = -2B_{12}$ and $\omega_0^2 = -r_0(r_0 + \sigma)$. Then, straightforward but tedious calculations show that

$$\begin{aligned} g_{20} &= \frac{\sigma}{2\omega_0} \left[\left(\frac{\omega_0}{\sigma} - \frac{r_0}{\sigma} i \right) \sigma_1 - i\sigma_2 \right] \\ &= A_{20} - 2B_{20} - \frac{2B_{20}}{\sigma} r_0 - \frac{i}{\omega_0} \left(\frac{2B_{20}}{\sigma} r_0^2 + (A_{20} + A_{11} + 3B_{20}) r_0 + \sigma B_{20} \right), \\ g_{11} &= \frac{\sigma}{2\omega_0} \left[\left(\frac{\omega_0}{\sigma} - \frac{r_0}{\sigma} i \right) \nu_1 - i\nu_2 \right] = A_{20} - \frac{A_{11}}{\sigma} r_0 - \frac{i}{\omega_0} \left(-\frac{A_{11}}{\sigma} r_0^2 + (A_{20} + B_{20}) r_0 + \sigma B_{20} \right), \\ g_{21} &= \frac{\sigma}{2\omega_0} \left[\left(\frac{\omega_0}{\sigma} - \frac{r_0}{\sigma} i \right) \tau_1 - i\tau_2 \right] \\ &= 3A_{30} - 2B_{12} - \frac{2(A_{21} + B_{12})}{\sigma} r_0 + \frac{i}{\omega_0} \left(\frac{2(A_{21} - B_{12})}{\sigma} r_0^2 - (3A_{30} + A_{21} + 5B_{12}) r_0 - 3\sigma B_{30} \right). \end{aligned}$$

According to Hassard *et al.* [1981], we have

$$\begin{aligned} \operatorname{Re}(c_1(r_0)) &= \operatorname{Re} \left\{ \frac{i}{2\omega_0} \left(g_{20} g_{11} - 2|g_{11}|^2 - \frac{1}{3}|g_{02}|^2 \right) + \frac{1}{2} g_{21} \right\} \\ &= -\frac{1}{2\omega_0} [\operatorname{Re}(g_{20}) \operatorname{Im}(g_{11}) + \operatorname{Im}(g_{20}) \operatorname{Re}(g_{11})] + \frac{1}{2} \operatorname{Re}(g_{21}) \end{aligned}$$

$$\begin{aligned} &= -\frac{A_{11}^2 + 2A_{11}A_{20} + A_{11}B_{20} + 2B_{20}^2}{2\omega_0^2\sigma}r_0^2 + \frac{2(A_{20}^2 + A_{20}B_{20} - 2B_{20}^2) + A_{11}(A_{20} - B_{20})}{2\omega_0^2}r_0 \\ &\quad - \frac{A_{21}}{\sigma}r_0 - \frac{B_{12}}{\sigma}r_0 + \frac{\sigma B_{20}(A_{20} - B_{20})}{\omega_0^2} + \frac{3}{2}A_{30} - B_{12} \\ &= -\frac{1}{r_0 + \sigma}A_{20}^2 + \frac{r_0}{2(r_0 + \sigma)\sigma}A_{11}^2 + \frac{2r_0 - \sigma}{2(r_0 + \sigma)\sigma}A_{20}A_{11} - \frac{1}{r_0}A_{20}B_{20} + \frac{1}{2\sigma}A_{11}B_{20} \\ &\quad + \frac{r_0 + \sigma}{r_0\sigma}B_{20}^2 + \frac{3}{2}A_{30} - \frac{r_0}{\sigma}A_{21} - \frac{r_0 + \sigma}{\sigma}B_{12}. \end{aligned}$$